ACS APPLIED BIO MATERIALS

www.acsabm.org Article

Surface Biochemical Modification of Poly(dimethylsiloxane) for Specific Immune Cytokine Response

Etienne Laborie,* Fabien Bayle, David Bouville, Claire Smadja, Elisabeth Dufour-Gergam, and Mehdi Ammar

Cite This: *ACS Appl. Bio Mater.* 2021, 4, 1307−1318 Read Online

ACCESS | Metrics & More | Article Recommendations | Supporting Information

ABSTRACT: Recent evidence suggests that proinflammatory cytokines, such as tumor necrosis factor α (TNF-α), play a pivotal role in the development of inflammatory-related pathologies (covid-19, depressive disorders, sepsis, cancer, etc.,). More importantly, the development of TNF-α biosensors applied to biological fluids (e.g. sweat) could offer non-invasive solutions for the continuous monitoring of these disorders, in particular, polydimethylsiloxane (PDMS)-based biosensors. We have therefore investigated the biofunctionalization of PDMS surfaces using a silanization reaction with 3-aminopropyltriethoxysilane, for the development of a human TNF-α biosensor. The silanization conditions for 50 μm PDMS surfaces were extensively studied by using water contact angle measurements, electron dispersive X-ray and Fourier transform infrared spectroscopies, and fluorescamine detection. Evaluation of the wettability of the silanized surfaces and the Si/C ratio pointed out to the optimal silanization conditions supporting the formation of a stable and reproducible aminosilane layer, necessary for further bioconjugation. An ELISA-type immunoassay was then successfully performed for the detection and quantification of human TNF-α through fluorescent microscopy, reaching a limit of detection of 0.55 μg/mL (31.6 nM). Finally, this study reports for the first time a promising method for the development of PDMS-based biosensors for the detection of TNF-α, using a quick, stable, and simple biofunctionalization process.

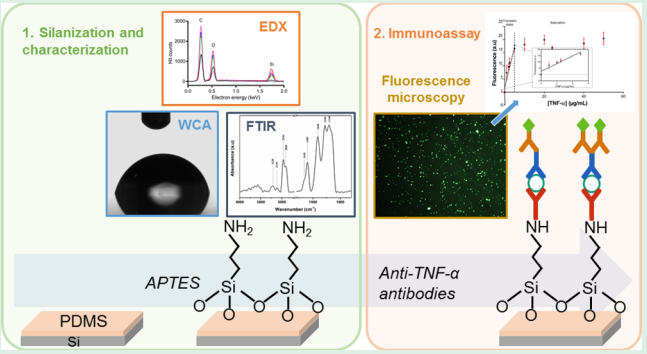

KEYWORDS: *silanization, PDMS, surface characterization, APTES, biosensor, TNF-α, antibodies, functionalization*

1. INTRODUCTION

Inflammatory-related diseases are among the leading causes of disease burden in the world.[1,2] For instance, patients suffering from major depressive disorders demonstrate an inflammatory response with increased levels of cytokines and chemokines in the blood and the brain.[3,4] Studies have shown that tumor necrosis factor α (TNF-α), interleukin 6 (IL-6), interleukin 1-β (IL-1β), and C-reactive protein are the most reliable biomarkers of inflammation.[5−7] In particular, TNF-α is involved in many inflammatory diseases such as arthritis, Crohn's disease, psoriasis, sepsis, pulmonary disorders, heart failures, covid-19, etc.,[6−9] Therefore, being able to capture and quantify it in various biological fluids (blood, sweat, saliva, etc.,) could greatly benefit the monitoring of many pathologies. Very few sensors have been targeting cytokines for health applications,[10−12] focusing on interleukin-6[13,14] and TNF-α[10−12,15−19] with electrochemical sensing on inorganic materials.

For improved analysis quality, biosensors can be integrated into a lab-on-chip or microchip for analyte collection, transport, and low-volume reactions.[20−22] To this day, polydimethylsiloxane (PDMS) remains one of the most used materials for microfluidics, thanks to its biocompatibility, flexibility, low cost, and ease-of-use.[23] However, using PDMS comes with trade-offs as pristine PDMS is known for its hydrophobicity causing a strong adsorption of biomolecules. A variety of processes has been developed[24−27] either for surface property modifications (hydrophobicity change and molecule absorption prevention) or molecular grafting.

Only a minority of devices include a biosensitive surface inside a microfluidic channel as it requires a reproducible and stable surface chemistry for biomolecule conjugations. Silanization reactions have been shown to be a convincing method for PDMS bonding,[28−30] surface modification for molecular grafting,[27,31−33] or even for preventing biofouling.[34] Silanization of PDMS relies on readily producible silanol groups for covalent bonding of silane molecules. Among the

Received: September 16, 2020
Accepted: January 12, 2021
Published: January 23, 2021

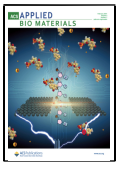

https://dx.doi.org/10.1021/acsabm.0c01188
ACS Appl. Bio Mater. 2021, 4, 1307−1318

available silanes, 3-aminopropyltriethoxysilane (APTES) is a well-known and commercially available reagent with a terminal amine allowing conjugation with biomolecules. A proper grafting of APTES on the PDMS surface offers stable free amine functions that could be used for bioconjugation with various molecules such as antibodies, enzymes, and DNA and RNA-based molecules.[35] The versatility of the developed platform can therefore benefit multiple lab-on-chip applications.

Several studies have used APTES for PDMS functionalization in its pure form[30,36] or by diluting in different solvents.[33,35,37−41] However, the silanization reaction is rarely controlled and only used as a surface preparation step. Developing a sensitive and reproducible detection surface is of paramount importance for human TNF-α detection considering its very low level in biological samples (~0.5 pM for sweat). Silanization reactions are highly sensitive reactions as APTES and silanes, in general, react very easily with water through a polymerization reaction, which is, most of the time, undesirable to obtain a clean and homogenous silane layer with readily accessible amine groups.[42] Therefore, conditions have rarely been optimized to reach a quality silane layer necessary for further bioreactions. Previous works, including ours, have followed a similar approach but were focused on silicon silanization and detection of different biological targets.[38,39,43]

While some studies have been using APTES on PDMS without prior activation of the surface,[32,44] it has been shown that activating the PDMS surface right before silanization would increase the grafting efficiency.[45,46] To the best of our knowledge, no comprehensive study related to controllable and stable direct PDMS silanization by APTES has been proposed.

In this study, the PDMS functionalization process by APTES has been deeply investigated for the first time. An extensive characterization of the surface properties has been performed to ensure reproducibility and quality of the modified surface. This paper reports an investigation of the biofunctionalization of a PDMS surface through an amino−silanization reaction with APTES toward a highly controlled integration process on biosensors. We have also investigated the correlation between controllable silanization and surface biofunctionalization. This study has been applied to human TNF-α detection. The following work aims to provide a quick, simple, and efficient approach for PDMS functionalization with nondestructive characterization techniques for promising applications in TNF-α detection and quantification.

2. MATERIALS AND METHODS

2.1. Materials. PDMS elastomer kit Sylgard 184 was obtained from Dow Corning. Ethanol 99%, acetone, and isopropyl alcohol of VLSI grade were obtained from Technic France. APTES, bovine serum albumin (BSA), fluorescamine (>98% TLC), phosphate buffer saline, Tween 20, animal-free recombinant human TNF-α, mouse monoclonal antihuman-TNF-α, FITC-tagged antimouse IgG, and FITC-conjugated antigoat IgG Fc specific and goat polyclonal antiporcine TNF-α were all obtained from Sigma-Aldrich Co. 2 in. silicon wafers were obtained from BT Electronics.

2.2. Silanization of PDMS. *2.2.1. Thin Film Preparation and Silanization.* PDMS samples and silanization were prepared as described previously[47] (see Figure 1). Samples were split in four equal pieces using a diamond cutter before silanization for characterization studies and in eight equal pieces for antibody grafting and immunocapture.

2.3. Wettability Measurements. The wettability measurements were done using the apparatus and procedure described previously.[47]

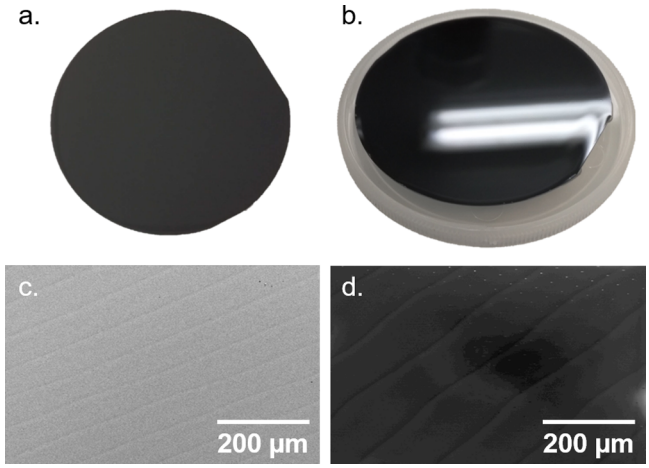

Figure 1. (a) Picture of a 2 in. Si wafer, (b) picture of a 2 in. Si wafer with a spin-coated 50 μm PDMS layer, (c) SEM picture of a 2 in. Si wafer, (d) SEM picture of a 2 in. Si wafer with a spin-coated 50 μm PDMS layer.

2.4. Energy Dispersive X-ray Spectroscopy Analysis. Energy dispersive X-ray spectroscopy (EDX) measurements were carried out using the same apparatus described previously.[47]

2.4.1. Silanization Condition Study. Samples were analyzed using the same conditions as in previous work.[47] The EDX values were averaged from five measurements at different locations on the sample with an analysis window of 1 mm × 500 μm. Noran System Six software was used for data collection and analysis. Net counts of X-rays were used for comparing samples and conditions instead of the atomic percentage given by the software as theoretical attribution models traditionally used for the identification are based on inorganic reference samples which would have a very different structure than a polymer.

2.4.2. Investigation of the Silane Layer on Selected Silanization Conditions. For a specific study of the silane layer on PDMS samples, different observation conditions were used to enhance the silane signal by grazing the surface. Samples were analyzed at 5 kV (10^{-5} mbar, Low Acceleration Bias) at 3.2 nA as probe current. Peak counts were averaged from five measurements distributed along the surface. Three tilt positions were tested: 0, 30, and 45° tilt. Noran System Six software was used for data collection and analysis. Net counts of X-rays were used for comparing samples and conditions instead of the atomic percentage given by the software, as explained in the previous section.

2.5. Fourier Transform Infrared Spectroscopy. Fourier transform infrared spectroscopy (FTIR) measurements were performed on a the same apparatus as in ref 39. All analysis areas were defined with the microscope prior to FTIR measurements. Results were then treated with the Varian Resolutions Pro software. The sample with a 50 μm PDMS layer treated with oxygen plasma was used as the background and subtracted from the silanized samples spectra.

2.6. Fluorescamine Detection and Fluorescence Microscopy. Free amine identification on silanized PDMS samples was done using a fluorescamine solution at 2 mg/mL in acetone. 250 μL of that solution were mixed with 2.25 mL of PBS (1X). Silanized samples were then immersed in the solution for 1 min. Samples were then washed three times with PBS (1X) and dried before being observed. Fluorescence microscopy was carried out on a large-field-inversed fluorescence microscope (Axio Observer, Zeiss) with a 10× magnification and acquisition time of 160 ms at 385 nm excitation and 475 nm emission. Quantification of fluorescent signals on PDMS samples was done using Icy software . Three pictures were collected per sample. The mean fluorescence intensity was calculated for each picture. Two intensity thresholds were then defined: a low-end filter to cut the background noise that could be attributed to potential

https://dx.doi.org/10.1021/acsabm.0c01188
ACS Appl. Bio Mater. 2021, 4, 1307−1318

shadows or light aberration occurring in the microscope; a high-end threshold to cut out the most intense points of the picture that could be attributed to aggregation of silanes or fluorophores. Based on this procedure, most of the information was conserved; only the most aberrant pixels are taken out. Fluorescence intensities were averaged on three pictures per sample, and standard deviation (SD) was calculated to assess the repeatability of the fluorescence detection. The mean square error (MSE) was also calculated to assess the homogeneity of the fluorescence intensity on the surface for each picture.

2.7. Antibody Grafting on Silanized PDMS Surfaces and Concentration Studies for Immunocapture. *2.7.1. Concentration Study for Primary Antibody Grafting.* All experiments have been carried out in a clean room environment on the 1 cm^2 surfaces previously silanized and using triplicates. Plasma-treated PDMS without exposure to silane were used as control samples. Diluted mouse monoclonal antihuman TNF-α antibody solutions were mixed with 100 μL of EDC (5 mg/mL) and 100 μL of S-NHS (8 mg/mL). 200 μL of antibody solutions was deposited on the silanized PDMS surfaces and left at 4 °C overnight in a glass container on an orbital shaker under medium stirring. The samples were rinsed five times with PBS containing 0.05% Tween 20. Surfaces were then blocked with a solution of PBS, 2% BSA solution for 2 h at room temperature (20 °C), then washed five times with PBS containing 0.05% Tween 20, and carefully dried under nitrogen. 200 μL of a solution of FITC-conjugated antimouse IgG (1:100) was added on the surface and left to react for 2 h at room temperature. Samples were then washed five times with PBS and Tween 20 (0.05%), one time with PBS, and one time with deionized water. Samples were then dried with nitrogen before observation with a fluorescent microscope.

2.7.2. Concentration Study for Human TNF-α Immunocapture. All experiments have been carried out in a clean room environment on the previously silanized 1 cm^2 surfaces and in triplicates. Samples were grafted with mouse monoclonal antihuman TNF-α following the previous process at a concentration of 1.0 μg/mL. The samples were rinsed five times with PBS containing 0.05% Tween 20. Surfaces were then blocked with a solution of PBS, 2% BSA solution for 2 h at room temperature (20 °C), then washed five times with PBS containing 0.05% Tween 20, and carefully dried under nitrogen. 150 μL of diluted human TNF-α solutions in PBS was added to the surface for immunocapture for 2 h at room temperature. The samples were rinsed five times with PBS containing 0.05% Tween 20. 150 μL of diluted goat polyclonal antiporcine TNF-α antibodies at 10 μg/mL in PBS and Tween 20 (0.05%) was added to the surface as detection antibody[48] and left to react for 2 h at room temperature. The samples were rinsed five times with PBS containing 0.05% Tween 20. 150 μL of diluted FITC-conjugated antigoat IgG (100 μg/mL) was added to the surface and left to react for 2 h at room temperature. Samples were then washed five times with PBS and Tween 20 (0.05%), one time with PBS, and one time with deionized water. Samples were then dried with nitrogen before observation with a fluorescent microscope.

2.7.3. Control Experiments on Bare PDMS, Blank Sample, and Control Sample without Primary Antibodies. For the comparison of bare PDMS and APTES-modified PDMS, samples followed the same protocol as previously described using a primary antibody concentration of 1 μg/mL. TNF-α was added at a concentration of 1 μg/mL. Detection antibodies and FITC-conjugated antibodies were used at 1 μg/mL and 10 μg/mL, respectively.

For the study of the APTES-modified samples without primary antibodies, samples followed the same protocol. Two sets of samples were studied with a TNF-α concentration of 1 and 5 μg/mL, respectively. Detection antibodies were used at 1 and 10 μg/mL. FITC-conjugated antibodies were used at 10 and 100 μg/mL.

A blank sample with 0 μg/mL of human TNF-α followed the same protocol with detection antibodies and fluorescent antibodies at 1 and 10 μg/mL, respectively.

2.8. Fluorescence Microscopy on Functionalized PDMS Surfaces with FITC-Tagged Antibodies. Microscope observations were realized with the same microscope setup as in Section 2.6 but with an acquisition time of 1500 ms at 475 nm exc. Five pictures per sample were taken for the different experiments. Mean fluorescence intensities and mean square error were calculated for each picture. SD was calculated between the replicates' fluorescence response.

Quantification of fluorescent signals on functionalized PDMS samples with FITC-tagged antibodies was done using Icy software. See Supporting Information for more details about the image treatment.

2.9. Statistical Analysis. All data were expressed as mean ± SD. A Mann−Whitney test was used to determine statistical significance between groups. A p-value of less than 0.05 was taken as meaningful difference.

For the silanization condition screening study, mean values and SD were calculated based on 10 points per sample for WCA and 5 points per sample for EDX analysis.

For the EDX tilt study, mean values and SD were calculated based on 5 points per sample.

For antibody grafting and immunoassay, experiments were carried out using triplicates. Mean fluorescent intensities and SD were calculated based on 5 pictures per sample.

3. RESULTS AND DISCUSSION

3.1. Silanization and Characterization of the Modified PDMS Surface. *3.1.1. Screening Study of the Silanization Conditions.* 50 μm-PDMS surfaces were prepared in a clean room environment according to a highly controlled process. Thin-film preparation control is critical for obtaining flat and homogeneous surfaces. Wafers were spin-coated with a 10:1 PDMS mix at 1000 rpm during 90 s on a spin-coater and then cured at 75 °C during 1 h in an oven. A targeted thickness of 50 μm was obtained with a ±1 μm accuracy, as verified by a mechanical profilometer.

To prepare PDMS films for silanization, substrates were treated with oxygen plasma (160 W, 0.4 mbar) for 1 min to create silanol groups on the surface. Silanization with APTES was performed at a constant humidity rate (1−5%), temperature (22 ± 1 °C), and pH (pH 7 to 8) at various concentration in ethanol and various reaction times from 15 min up to 1 h. Samples were then rinsed and dried.

Characterization of surface modification on PDMS is usually done using the water contact angle (WCA), X-ray photoelectron spectroscopy (XPS), and Fourier transform infrared (FTIR) spectroscopy.[24,49] WCA and FTIR analyses do not require any sample preparation, being quick and easy to carry out and giving important information about the surface properties and chemical composition of the surface. XPS analysis allows a precise investigation of the surface elements and their respective oxidation state for the first few nanometers. However, the very strict vacuum conditions and surface state ($<10^{-5}$ Pa)[26,31] are not always compatible with silicon polymers that outgas inside the chamber[50] and require a very rigorous sample preparation procedure. On the other hand, EDX gives information about the elements in the first few microns of the surface, giving atomic distribution of the sample (without oxidation states), under milder vacuum conditions ($\sim 10^{-3}$ Pa). Finally, it can be done easily and quickly (~15 min per sample) within a standard SEM installation without sample pretreatment, which is an important aspect to consider for screening different preparation conditions of APTES-modified PDMS samples. Very few studies have used EDX analysis for PDMS and silanes but it allowed discrimination of APTES within PDMS-coated nanoparticles for functionalization,[51] cell membrane analysis from a PDMS-base microfluidic cell culture,[52] and APTES-modified PDMS surface analysis before metal deposition.[28] Finally, EDX is an easy-to-use and fast technique, allowing for

https://dx.doi.org/10.1021/acsabm.0c01188
ACS Appl. Bio Mater. 2021, 4, 1307−1318

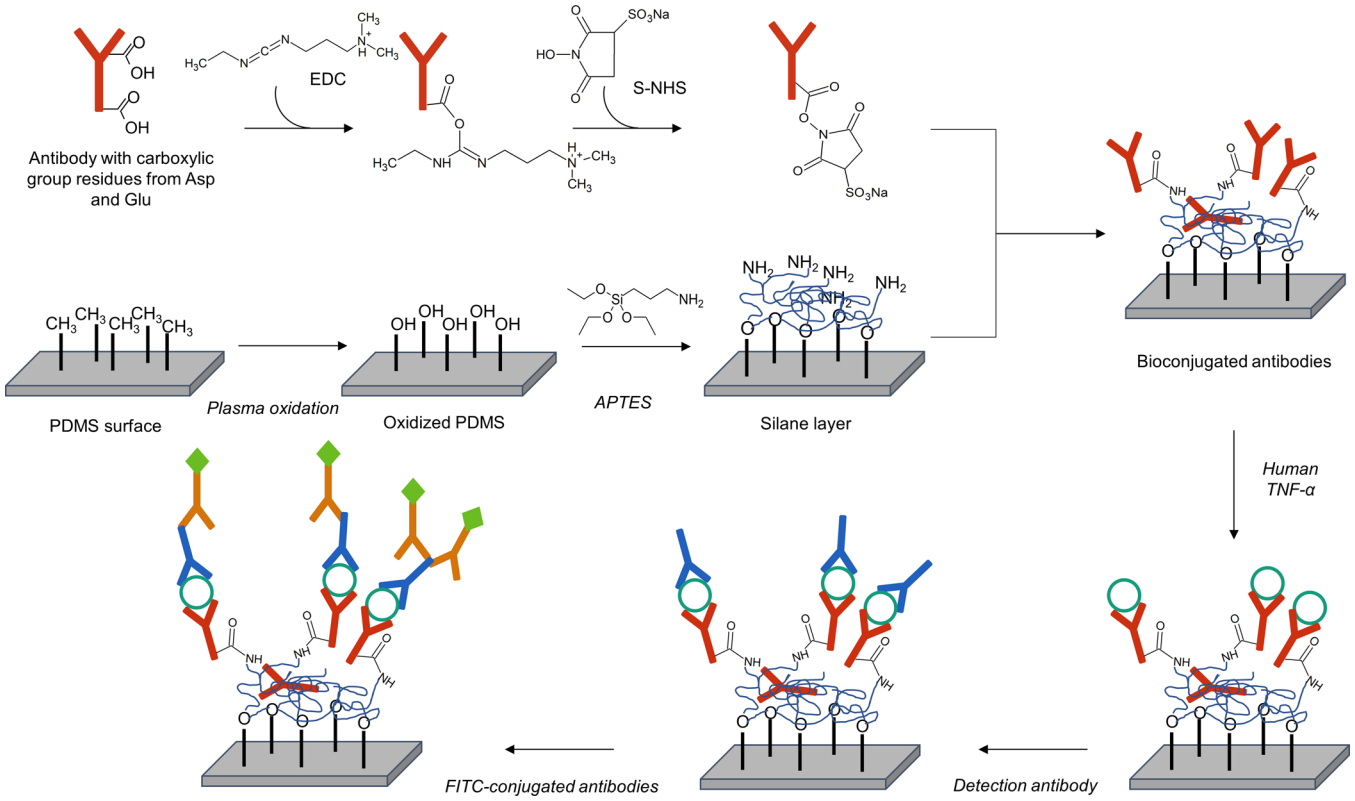

Figure 2. Schematic representation of the PDMS surface functionalization process followed by the immunocapture and detection of human TNF-α.

a semi-quantitative analysis of surface modification. In this study, we used a combination of WCA, EDX, FTIR, and fluorescent microscopy to characterize the silanized surfaces.

Bioconjugation between immobilized APTES molecules and antibodies is done by creating an amide bond using EDC (*N*-(3-dimethylaminopropyl)-*N*′-ethylcarbodiimide hydrochloride) and S-NHS (*N*-hydroxysulfosuccinimide sodium salt) coupling with the aspartate and glutamate amino acids inside the antibody structure (see Figure 2). S-NHS is used to improve the solubility and stability of the active ester intermediate in aqueous solutions, increasing the conjugation reaction yield.[53]

Wettability measurements were performed to follow the modification of the surface after plasma oxidation and silanization. PDMS is a hydrophobic polymer once it is cured (116.6 ± 0.7°, see Table S1 in Supporting Information). Through O_2 plasma treatment, the surface becomes temporarily hydrophilic with a very low contact angle (<5°), below the software measurement limit (see Table S1), due to the creation of silanol groups. Plasma treatment is needed for surface activation, and several studies have reported the modifications induced by plasma treatment on PDMS samples.[54−56] The silanol groups created on the surface allow for a condensation reaction to occur with silane molecules, improving the grafting of APTES on the polymer. Without plasma activation, very few hydroxyl groups would be available and APTES molecules would be weakly bonded to the surface.

Following silanization, contact angles were measured 24 h after reaction to allow the surface to stabilize as significant changes occur in the silane density during the first hours after reaction. The presence of the amine groups and the carbon chains of APTES resulted in a more hydrophobic surface with higher contact angles varying from 70 to 90° (see Figure S1), in agreement with the value range from the literature for the APTES-modified PDMS surface.[37,44,57,58] These values support the modification of a hydrophobic surface (WCA > 90°) toward a more hydrophilic one (WCA < 90°), whose behavior would vary depending on silane molecule orientation and reorganization as APTES molecules have both hydrophilic ($-NH_2$) and hydrophobic (carbon chain) parts. Reference measurements on the plasma-treated sample immersed in ethanol without APTES were carried out. WCAs tend to be lower than silanized surfaces (72.7 ± 16.6°, see Table S1) but higher than plasma-treated PDMS. Due to hydrophobicity recovery of PDMS, the surface of the control sample is covered with $-SiO_x-$ (x = 3−4), $-Si(O,CH_3)-O$, and $Si(OH)_2-O$ groups which tends to both decrease and increase hydrophobicity.[59] High SDs observed in Figure S1 can be explained by the plasticity of the polymer materials. Native PDMS samples tend to have a random surface structure that would affect the chemistry of the following functionalization treatment. In our case, PDMS sample preparation was highly controlled in order to minimize the heterogeneity of the surface on each sample as well as the variability among the different prepared samples. The entire process was carried out inside a clean room facility, with an industrial spin-coater, after carefully mixing and degassing the PDMS mix. The cured PDMS samples were characterized with WCA and AFM. Very little variations were observed along the surface of the sample (surface roughness less than 2 ± 0.1 nm, see Figure S2 in Supporting Information), offering a stabilized starting material before chemical modifications.

Several studies have reported the mechanisms involved in the hydrophobic recovery of the polymer after plasma

https://dx.doi.org/10.1021/acsabm.0c01188
ACS Appl. Bio Mater. 2021, 4, 1307−1318

treatment.[54−56] This behavior would affect the surface state of the sample, possibly degrading the first chemical modifications brought by the silanization reaction. APTES molecules would suffer from the surface reorganization at first but would stabilize with time as silane layers start to build. Reaction times of less than 45 min induced significant shifts in hydrophobicity. Contact angles were less affected by variations in APTES concentration but nonetheless surfaces became significantly more hydrophilic at low concentrations (10−20%) and short reaction times. As supported by the first WCA screening study, favorable silanization conditions could be obtained with a reaction time of 30 min and APTES concentrations of 10−20%.

Further investigation of silanization was made using EDX analysis, as a semi-quantitative method for investigating polymer surfaces. EDX allows the determination of atomic distribution in the first few microns of the surface. Regarding our analysis, three atoms were detected in various amounts: C, O, and Si (see Figure 3). A low voltage of 3 kV was used for analysis in order to prevent overcharging the surface, resulting in a more reliable analysis. Nitrogen was expected at first to be detected, but its low relative abundance within the sample (<3%) and its low energy of the K shell (0.392 keV) make it hard to detect with a standard electron detector as energy resolution between C, N, and O remains an issue.[60] Nitrogen atoms could be expected only in the very first nanometers of the surface with a very superficial analysis, although these first molecular layers would have highly variable molecular conformations, making it hard to confirm element detection and exclude contamination. The investigation of nitrogen to support the presence of amine functions on the surface is more accurately done and validated with the fluorescamine and FTIR analysis in part 3.1.2. Therefore, only carbon, oxygen, and silicon amounts were studied by EDX measurements.

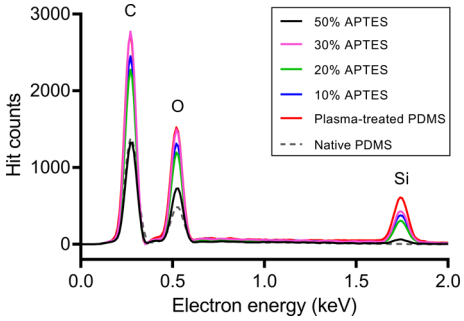

Figure 3. EDX spectrum of native, plasma-treated, and silanized PDMS samples: silanization has been performed for 30 min at different concentrations of APTES in ethanol.

Figure 3 shows the EDX spectrum of several PDMS samples with corresponding peaks for C, O, and Si K shells. Heights of peaks allow for quantification of atom relative abundance within the samples. Native PDMS shows a very low level of silicon, whereas plasma-treated PDMS shows the highest amount of Si. Silanized samples shows a variation of these components as the APTES concentration varies.

Zhang et al.[28] used a similar approach for characterizing PDMS surfaces silanized with APTES before metal deposition. They also used WCA analysis but obtained unexpected results with a 55 ± 10° angle on pristine PDMS. PDMS is known for being highly hydrophobic, and WCAs should be measured above 100° as previously explained. Concerning EDX measurements, they analyzed the amount of C, O, and Si on PDMS and APTES-modified PDMS but obtained very different results from the two samples. Silicon and carbon contents differ from our analysis which could be explained by different analysis conditions, considering that the paper is not mentioning the conditions used for EDX measurements, as well as the use of the theoretical model for atomic quantification. We used direct hit counts instead of the atomic percentage from the software as the structure of reference samples in the software model is usually an inorganic sample while our analysis refers to an organic polymer. Our study offers a more comprehensive approach for the understanding of the mechanism involved in the formation of the clean silane layer.

To characterize the quality of the silanization reaction, regarding the surface state and successful silanes grafting on PDMS, we evaluated the quality of the silane layer by following the variation of the ratio between Si and C (Si/C). A good quality silanization is characterized by a high amount of silane on the surface, organized as a single layer of molecules, with a good homogeneity in the repartition of molecules on the surface. Pristine PDMS ($-[O-Si(CH_3)_2]_n-$) is mostly composed of carbon. In methyl groups ($-CH_3$) having a high steric hindrance, incoming electrons would hit carbon in majority. Through EDX analysis, pristine PDMS would therefore show an increased carbon amount with a drop signal from silicon as few electrons would hit silicon, and a lower Si/C ratio could be expected. After plasma treatment, the methyl groups are replaced by silanol groups with relatively lower steric hindrance and therefore allow silicon to be detected, while diminishing the carbon amount on the surface. The Si/C ratio is then expected to rise as Si increases and C decreases. However, APTES ($C_9H_{23}NO_3Si$) has also a high amount of carbon due to the carbon backbone and some silicon. Successful grafting of APTES with vertical silane orientation would therefore reach an equilibrium state before surface overloading with more APTES molecules. The Si/C ratio is expected not to vary significantly, but with more APTES molecules, electrons would be prevented from hitting silicon and Si contribution would decrease while increasing C. The Si/C ratio is expected to decrease slightly but variations of the silane arrangements on the surface would yield varying Si/C ratios, represented by high SDs on Figure 4.

Figure 4 shows a graphic evolution of the Si/C ratio according to different reaction conditions. No X-ray from silicon was observed for pristine PDMS, yielding a very low Si level. The highest ratios are obtained with short times (<45 min) and moderate concentrations of APTES (10−20%). High reaction time (>45 min) and concentrations over 30% yield to a Si/C ratio decrease probably due to surface overloading with APTES molecules. A high amount of APTES molecules in solution yields a higher steric hindrance close to the surface, therefore preventing more molecules to react with silanol groups. This could be explained by the first silane layer covered with other APTES molecules linked with weaker bonds through electrostatic interactions from the amine and hydroxyl functions as well as van der Waals interactions from the carbon backbone. The higher amount of carbon and lower amount of silicon demonstrate that the signal from silicon is screened by the carbon signal from the carbon backbone of APTES. High amounts of APTES are detrimental to the homogenous silanization of the surface with amine groups available for further conjugation. It is probable that short reaction times

https://dx.doi.org/10.1021/acsabm.0c01188
ACS Appl. Bio Mater. 2021, 4, 1307−1318

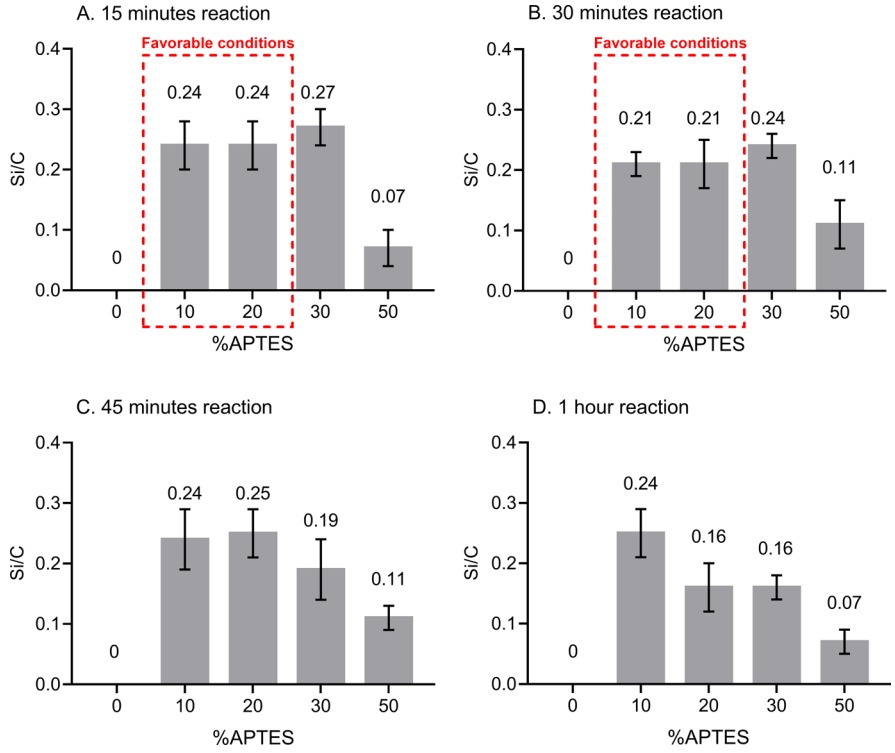

Figure 4. Evaluation of Si/C ratio as a function of APTES concentration (0, 10, 20, 30, and 50% in ethanol) for different reaction times with EDX analysis: A: 15 min, B: 30minutes, C: 45 min, and D: 1 h 0% APTES sample correspond to native PDMS with no plasma activation and immersed in pure ethanol during the reaction time. Tilt angle used: 0°.

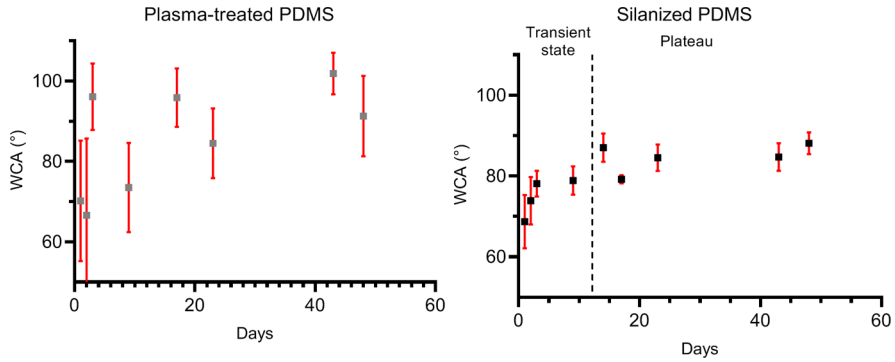

Figure 5. WCA measurements on various PDMS samples at different ageing times after plasma-treatment (left) and silanization reaction with 20% APTES for 30 min (right). Points plotted do not necessarily belong to the same aged PDMS sample; several measurements at various times were pooled.

(<15 min) did not allow the grafting of enough amine groups on the surface and most silane molecules would be weakly linked to the surface through noncovalent interactions. On the other hand, long reaction times (>45 min) probably cause surface overloading which tend to decrease the silane layer quality.

From Figure 4, favorable silanization conditions can be selected (see red boxes), allowing enough time and silane molecules to react with the silanol groups on the PDMS surface without showing signs of degradation through a decrease of the Si/C ratio or an increase in its SD. No significant differences ($p > 0.05$) could be noted for reactions shorter than 30 min and concentrations below 30%. We concluded that low APTES concentrations (<30%) and short reaction times (between 15 and 30 min) are more suitable to prevent surface overloading with APTES molecules, diminishing amine function availability for further reaction with proteins. Finally, the EDX study needs to be considered within the whole strategy including the WCA analysis. WCA and EDX screening studies pointed out that a significant degradation of the silanization quality occurs after 45 min of reaction and a silane concentration higher than 30%.

From the region corresponding to the favorable conditions for the PDMS silanization, we selected our reaction time to be 30 min with 20% APTES, offering enough time and available silane molecules for the reaction to reach an equilibrium state without risking silane aggregation.

3.1.2. Study of the Silane Layer Quality in the Selected Silanization Conditions. After screening the different silanization conditions of PDMS surfaces, the selected conditions were more thoroughly characterized to better qualify the silane layer and amine function availability.

https://dx.doi.org/10.1021/acsabm.0c01188
ACS Appl. Bio Mater. 2021, 4, 1307−1318

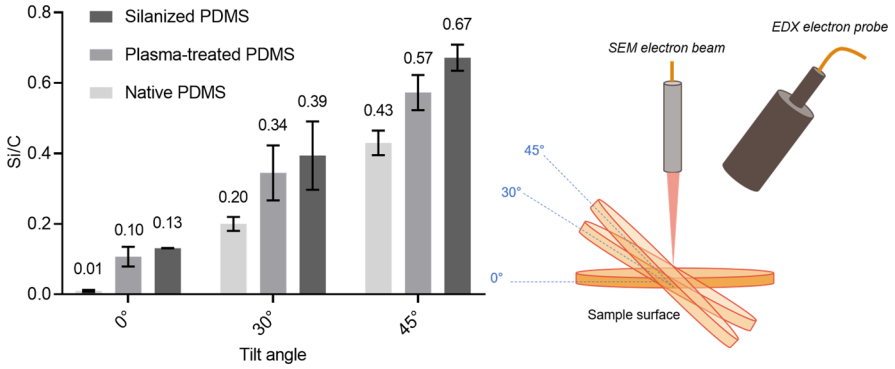

Figure 6. Left: Impact of tilting during EDX analysis of various PDMS samples: native PDMS, plasma-treated PDMS and silanized PDMS (20% APTES, 30 min). Right: Schematic of the tilted positions of the sample inside the SEM chamber with respect to the electron beam and EDX probe.

Setting the APTES concentration and reaction time to 20% and 30 min, a more thorough and extensive investigation of the surface was done using WCA and EDX. Stability of different samples was evaluated over a period of 45 days with WCA (see Figure 5). After silanization, WCAs on silanized surfaces reached 68.7 ± 6.6°, compared to 70.2 ± 15.0° for plasma-treated samples, demonstrating a more hydrophilic behavior of the surfaces due the amine functions of the silane. Over the days, this behavior declined as the silanized samples recovered some hydrophobicity but seemed to stabilize at an 85° WCA while plasma-treated-only samples behave more randomly, recovering most of their hydrophobicity over seemingly random times. This highlights that plasma-treated and APTES-modified PDMS surfaces may undergo significant surface reorientation after a few days, but silanized samples remain globally stable, thanks to silane molecules. A similar behavior has been reported by Séguin et al. on PDMS modified with APTMS.[49] The initial WCA values over the first few days (~70°) characterize a more hydrophilic behavior of the surface, offering a good starting point for further biochemical reactions in the process.

Additionally, EDX measurements were performed with varying tilt positions of the characterized samples. By tilting the sample, we used a grazing angle condition to reach a more surface sensitive analysis and collect more information about the silane layer.[60] Native, plasma-treated and silanized PDMS samples were compared along three tilt positions: 0, 30, and 45°. Figure 6 shows the impact of the tilt on the Si/C ratio for the different PDMS samples.

From Figure 6, we can conclude that tilted EDX analysis allowed to bring out the differences between the different PDMS treatments. A grazing angle of analysis changes the diffusion cone of the electron in the sample, enabling more electrons from the upper layers to be excited and detected.[60] Electron-rich atoms like Si are then more visible while carbon contribution drop. Therefore, silanized PDMS showed a significantly ($p < 0.05$) higher Si/C ratio, especially at tilt 45°. Compared to the previous study on silanization conditions in Section 3.1.1, EDX analysis conditions were changed and optimized to enhance these differences. Here, a significant ($p < 0.05$) change occurred on the Si/C ratio after plasma-treatment and more importantly following silanization. At tilt 0, these differences are less striking and the Si/C ratio of plasma-treated and silanized PDMS is close but still significatively different ($p < 0.05$). However, by tilting the sample from 0 to 45°, it increased the contribution of the surface, allowing a better discrimination between the samples and a more accurate characterization of the silanization process. We could therefore highlight significant differences ($p < 0.05$) between native PDMS, plasma-treated PDMS and silanized PDMS at tilt 45°, supporting an adequate PDMS modification after silanization, and confirm the presence of a silane layer on the PDMS surface after silanization of the sample following the selected conditions from part 3.1.1.

Investigation of free amine availability and reactivity after silanization of the PDMS was done with fluorescamine. Fluorescamine reacts easily with free amines with a high specificity and gives qualitative and semi-quantitative information about the silane layer quality. In this experiment, freshly silanized PDMS samples (in the selected conditions from part 3.1.2) and control samples reacted with fluorescamine for 1 min. Figure S3 (see Supporting Information) displays images acquired with a fluorescent microscope. Quantification of the fluorescence intensity was performed after image processing. A mean fluorescence intensity of 144.41 au (MSE of 49.01) was obtained for silanized samples, whereas plasma-treated PDMS displays a fluorescence of 124.4 au [mean squared error (MSE) of 60.78]. This demonstrates that enough amine functions were created on the PDMS surfaces through silanization, allowing further conjugation with biomolecules, in comparison to control samples. The mean squared error (MSE) gives information about the homogeneity of the fluorescent signal on the surface. Fluorescence intensity variations on silanized samples could be attributed to variation in the silane conformation on the surface, affecting the primary amine availability for further reaction with fluorescamine. Several studies[35,61,62] have reported that different parameters could affect the organization of the silane molecules on the surface after silanization. Substrate topology, solvents, silane concentration, and processing could promote the formation of SAMs or multilayers with covalently bonded and weakly bonded molecules. The selected silanization conditions (APTES concentration, ethanol as solvent, and 30 min reaction time) would most likely result in a multilayer of interlaced molecules with free and bounded amines, causing a variable distribution of available primary amines along the PDMS surface. Moreover, as we previously explained in Section 3.1.1, PDMS plasticity could also affect the surface behavior and fluorescent response. Our main objective is to stabilize the contribution of the PDMS chemical structure to our functionalization process and render it as reproducible as possible. Control sample fluorescence values are mostly due to intrinsic fluorescence of PDMS.[63] This is illustrated by the higher MSE.

https://dx.doi.org/10.1021/acsabm.0c01188
ACS Appl. Bio Mater. 2021, 4, 1307−1318

As previously explained, amine functions are key for further bioconjugation on the surface. We used FTIR spectroscopy to validate the presence of the chemical environment of amine groups on the PDMS surface and confirm the appropriate functionalization with APTES.

Figure 7 shows a typical IR vibrational spectrum for PDMS pretreated with plasma and after APTES silanization using the optimal conditions (20% of [APTES] and 30 min of reaction). As expected, the hydroxyl group and hydrogen-bonded water molecule give a large band in the 3600 cm^{-1} region. In addition, the most relevant band is from 1100 to 1250 cm^{-1} which is relative to the Si−O−Si vibrational modes, certainly due the presence of the continuous silica layer as a background layer for silanes. The vibrational band at 1140 cm^{-1} should be assigned to the stretching mode in the growing layer created by APTES condensation reactions as confirmed in the literature.[64] Moreover, the NH_2 scissor vibration detected at 1580 cm^{-1} highlights significantly the amine functions from APTES. On the other hand, the features at 1640 cm^{-1} could be attributed to the symmetric and asymmetric $-NH_3^+$ deformation mode representatives of the protonated amine function occurring when silanes get in contact with air.[64,65] In the range of 3100−3300 cm^{-1}, a very weak vibrational band of asymmetric and symmetric −NH stretching modes of the amine groups is clearly identified, as mentioned in the literature.[66] CH_2 asymmetric and symmetric stretching modes are also observed at 2860 and 2930 cm^{-1}. Their presence could be related to the propyl chains from the carbon backbone of APTES, although the organic contamination of the native PDMS sample cannot be excluded.

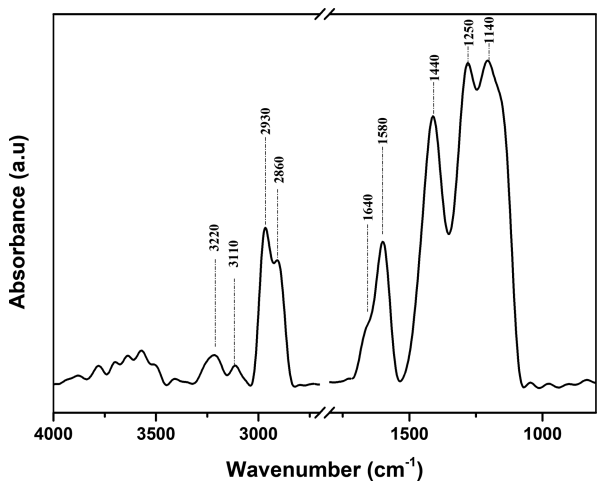

Figure 7. IR vibrational features of the amino-silanized PDMS using optimal conditions of treatment (20% of [APTES] and 30 min of reaction). Plasma-treated PDMS sample was used as the background and subtracted from silanized sample spectra.

Finally, the various analysis made with WCA, EDX, FTIR, and fluorescamine reaction gives a thorough validation for the creation of a stable amine-layer on the PDMS surface. Moreover, all the results point out to optimal silanization reaction conditions to reach a stable and reproducible amine-based molecular anchoring. The use of a variety of characterization techniques resulted in the better understanding of the modification induced on the sample's surface and helped clarify encouraging outcomes when such surfaces are used as biosensing platforms. The method presented here represents a rapid way of modifying and characterizing PDMS surfaces prior to bioconjugation. The following study uses the selected silanization conditions (20% APTES concentration in ethanol and 30 min reaction time) to functionalize PDMS surfaces with anti-TNF-α antibodies for immunocapture of the biomarker in solution relative to inflammatory-related pathologies.

3.2. Antibody Grafting on Functionalized PDMS Surfaces and Application to a Human TNF-α Immunoassay. To demonstrate the performance of the silanized PDMS surfaces, mouse monoclonal antihuman-TNF-α antibodies were grafted on the surface. Performance of bare PDMS and APTES-modified PDMS was compared. Then, the samples were tested for immunocapture of TNF-α following an immuno-sandwich strategy, as depicted in Figure 2.

3.2.1. Comparison of Bare PDMS with APTES-Modified PDMS and Assessment of the Immunocomplex Specificity. Before assessing the surface for its capture efficiency of various amounts of TNF-α, bare PDMS and APTES-modified PDMS were compared in the same conditions (with TNF-α at 1 μg/mL) following the grafting procedure described in 2.7.3. A low concentration of antigen was chosen for this experiment in order to assess the sensitivity of both surfaces, avoiding antigen saturation of the surface. Fluorescent intensities of 19.36 ± 0.24 and 17.88 ± 1.02 au were obtained for silanized and bare PDMS, respectively. SD of the fluorescent response along the bare PDMS was four times greater than silanized PDMS, meaning that silanization brings significant benefits to the immunosensing process. Indeed, it confers a more consistent and reproducible anchor for the grafting of the immunocomplexes, improving the biosensing performance and homogeneity of the response.

Additionally, a second and separate control experiment was performed to evaluate the signal of APTES-modified samples when no primary antibodies are immobilized on the surface.

Table 1. Fluorescent Microscopy Analysis of: (A) Control Samples Depending on Antigen and Detection/Fluorescent Antibodies Concentrations (B) Blank Sample

line #	sample type	surface type	primary anti-TNF-α antibody (μg/mL)	TNF-α concentration (μg/mL)	detection Ab concentration (μg/mL)	FITC Ab concentration (μg/mL)	mean fluorescent intensity ± SD (au)
			(A) Without a Primary Antibody Layer				
1	control sample	silanized PDMS with no primary antibody	0	1	1	10	17.31 ± 0.22
2	control sample	silanized PDMS with no primary antibody	0	5	10	100	16.42 ± 0.14
			(B) Without Antigen				
3	blank sample	silanized PDMS with primary antibody	1	0	1	10	18.86 ± 0.38

https://dx.doi.org/10.1021/acsabm.0c01188
ACS Appl. Bio Mater. 2021, 4, 1307−1318

Without a primary antibody layer, a fluorescence response of 17.31 ± 0.22 au was obtained (see Table 1A below) in the same conditions than the previous experiment, which can be imputed to the background noise measured on bare PDMS samples. Therefore, it was concluded that without a primary antibody layer, no antigen and no detection/fluorescent antibodies can be immobilized on the surface. The remaining fluorescent signal was attributable to absorption of one of these molecules in limited amounts. Moreover, antibody solution concentrations did not affect the resulting signal as shown by lines #1 and #2 of the table. These two control experiments support a good specificity of the immunocomplex between its components and a poor affinity for the bare PDMS surface.

Finally, these two experiments demonstrated that primary antibody affinity for amine functions will most definitely drive the complex to build on the silane molecules on the APTES-modified surface, whose presence has been validated in the previous study from part 3.1.

3.2.2. Grafting of Antihuman-TNF-α Antibodies on Silanized PDMS. To demonstrate the performance of the silanized PDMS surfaces, mouse monoclonal antihuman-TNF-α antibodies were grafted on the surface and detected with antimouse FITC antibodies. In order to determine the optimal concentration for the grating of a capture antibody layer on the surface, a calibration curve was plotted for the anti-TNF-α antibody concentration from 0 to 5 μg/mL. BSA was used to block nonspecific bindings of the fluorescent antibodies on the PDMS surface. Figure 8 shows the calibration curve with a linear range from 0 to 1.5 μg/mL. Fluorescence intensity seems to reach a maximum and to decrease slightly at high concentrations of antibodies as the surface is saturated with proteins and antibodies start to aggregate. A quenching effect could explain the slight intensity decrease at high concentration.[67] At lower concentrations, fluorescent intensity shows a linear behavior, with a maximum concentration at 1.5 μg/mL in the linear range. A working concentration around 1.0 μg/mL would offer a stable and sufficiently functionalized surface suitable for immunocapture without risking surface saturation and antibody aggregation. We demonstrated that the silanized PDMS samples show a linear response toward the grafting of anti-TNF-α antibodies which is the first critical step for immunocapture and detection of human TNF-α, as depicted in Figure 2. This must be considered as the first strong and reliable argument supporting the bioreactivity of the functionalized PDMS surface.

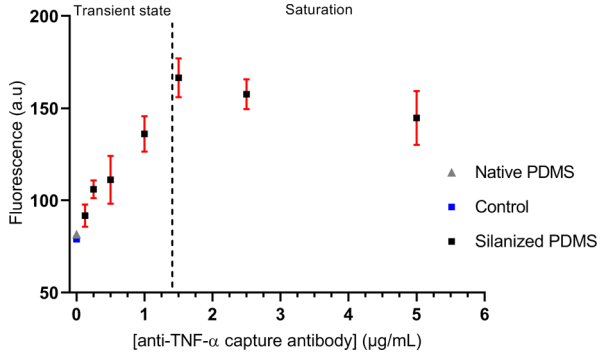

Figure 8. Fluorescence microscopy analysis of various capture antibody concentrations on silanized PDMS samples: eight concentrations of immobilized mouse monoclonal antihuman TNF-α were tested: 0 μg/mL (as control), 0.125, 0.250, 0.500, 1.00, 1.50, 2.50, and 5.00 μg/mL. Native (non-silanized) PDMS was tested as well.

3.2.3. Grafting of TNF-α Immunocomplex on Silanized PDMS. Immunocapture of various amounts of TNF-α was therefore investigated following the process depicted in Figure 2, with a working concentration of capture antibodies at 1.0 μg/mL according to the previous study. The Figure 9 inset shows the calibration curve of human TNF-α with a linear behavior over a concentration range of 0.5−5 μg/mL (determination coefficient being at 0.91). The blank sample was evaluated when no antigen is added to the surface with a primary antibody layer. A fluorescent response of 18.36 ± 0.38 au, similar to control experiment samples from Section 3.2.1, was obtained (see Table 1B), validating the fact that an incomplete immunocomplex shows a weak fluorescent response, identified as background noise. The blank sample signal was therefore subtracted from the samples in the following immunocapture study.

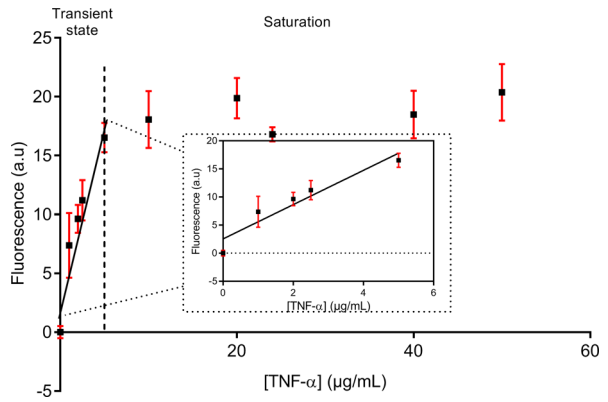

Figure 9. Fluorescence microscopy analysis of human TNF-α immunocapture on silanized PDMS samples. Human TNF-α concentrations varied between 0 and 50.00 μg/mL. Silanized PDMS with no antigen was used as the background sample.

The fluctuations observed at high concentrations can be attributed to the partial saturation of the binding sites on the surface and a possible quenching effect from the fluorophore.[67] The limit of detection (LOD) was evaluated at 0.55 μg/mL (i.e. 31.6 nM)[68] showing a satisfactory sensitivity of the surface. Other studies on TNF-α biosensing devices have reached a limit of detection between 20 pg/mL and 25 ng/mL using different detection methods known to be more sensitive than fluorescent detection (QCM,[17] electrochemical sensing[18]). Few studies have used fluorescent detection of TNF-α through antibody capture, and detection has been carried out in solution using microbeads or in microplates, sometimes not considering nonspecific absorption and washing steps.[69] Although the limit of detection is still high for accurate detection of TNF-α in sweat or blood samples (working concentrations are around ∼pg/mL[70]), using fluorescence detection offers a limited capacity for signal amplification compared to electrochemistry or magnetic sensors. Finally, it is important to note that even after a careful optimization of the functionalization and detection protocol, some inherent aspects of surface immunoassays can still hinder sensitivity and specificity, such as controlling the chemical stability of the surface and preventing nonspecific response as well as aggregation of biomolecules on PDMS. Nevertheless, this work is the first step for the integration of bioactive surfaces

https://dx.doi.org/10.1021/acsabm.0c01188
ACS Appl. Bio Mater. 2021, 4, 1307−1318

inside lab-on-chip devices for the development of biosensing applications.

4. CONCLUSIONS

In the present study, we performed, for the first time, a controlled and accurate silanization for PDMS surfaces with aminosilanes. Surfaces have been extensively characterized by WCA, EDX, FTIR, and fluorescamine detection. All results support the expected chemical modification of the surface with the presence of amine functions on the silanized PDMS surface compared to control samples, therefore providing a stabilized platform for antibody grafting and application to immunocapture. Grafting of anti-TNF-α antibodies on silanized PDMS was performed, and we evaluated the binding capacity of the surfaces with fluorescent microscopy. We then used the functionalized surfaces to capture human TNF-α in solution, reaching a LOD of 0.55 μg/mL (31.6 nM) which is promising considering the limited signal amplification provided by the fluorescent tag. Finally, the above study reports for the first time a promising method for the fabrication of a PDMS-based microfluidic sensor for human TNF-α using a highly controlled silanization process. Future work will address the application of amino-silanized PDMS for the covalent immobilization of anti-TNF-α antibodies inside microfluidic channels and detect human TNF-α in solution and artificial sweat. Therefore, we highlight promising results for the development of a biosensor for the quantification of TNF-α in human sweat, applied to inflammatory-related diseases continuous monitoring.

■ ASSOCIATED CONTENT

Supporting Information

The Supporting Information is available free of charge at https://pubs.acs.org/doi/10.1021/acsabm.0c01188.

Table of WCA measurements on silanized PDMS samples; bar graph of WCA measurements on PDMS samples for different silanization conditions; AFM measurements on a spin-coated PDMS surface; and fluorescent microscopy pictures for fluorescamine detection on silanized PDMS (PDF)

■ AUTHOR INFORMATION

Corresponding Author

Etienne Laborie − *Center for Nanosciences and Nanotechnologies, CNRS, Université Paris-Sud, Université Paris-Saclay, 91120 Palaiseau, France; Institut Galien Paris Sud, UMR 8612, Protein and Nanotechnology in Analytical Science (PNAS), CNRS, Université Paris-Sud, Université Paris-Saclay, 92290 Châtenay-Malabry, France;* orcid.org/0000-0003-3222-8299; Email: etienne.laborie@c2n.upsaclay.fr

Authors

Fabien Bayle − *Center for Nanosciences and Nanotechnologies, CNRS, Université Paris-Sud, Université Paris-Saclay, 91120 Palaiseau, France*

David Bouville − *Center for Nanosciences and Nanotechnologies, CNRS, Université Paris-Sud, Université Paris-Saclay, 91120 Palaiseau, France*

Claire Smadja − *Institut Galien Paris Sud, UMR 8612, Protein and Nanotechnology in Analytical Science (PNAS), CNRS, Université Paris-Sud, Université Paris-Saclay, 92290 Châtenay-Malabry, France*

Elisabeth Dufour-Gergam − *Center for Nanosciences and Nanotechnologies, CNRS, Université Paris-Sud, Université Paris-Saclay, 91120 Palaiseau, France*

Mehdi Ammar − *Center for Nanosciences and Nanotechnologies, CNRS, Université Paris-Sud, Université Paris-Saclay, 91120 Palaiseau, France*

Complete contact information is available at: https://pubs.acs.org/10.1021/acsabm.0c01188

Notes

The authors declare no competing financial interest.

■ ACKNOWLEDGMENTS

This work was supported by a public grant overseen by the French National Research Agency (ANR) as part of the "Investissement d'Avenir" program, through the CD IDEX-IDI 2017 project funded by the IDEX Paris-Saclay, ANR-11-IDEX-0003-02, and LabeX LaSIPS (ANR-10-LABX-0040-LaSIPS). The authors have declared no conflict of interest.

■ ABBREVIATIONS

PBS, phosphate buffer saline; WCA, water contact angle; PDMS, polydimethylsiloxane; APTES, 3-aminopropyltriethoxysilane; EDC, *N*-(3-dimethylaminopropyl)-*N*′-ethylcarbodiimide hydrochloride; S-NHS, *N*-hydroxysulfosuccinimide sodium salt; EDX, energy dispersive X-ray spectroscopy; FTIR, Fourier transform infrared spectroscopy; XPS, X-ray photoelectron spectroscopy; MDD, major depressive disorders; TNF-α, tumor necrosis factor α; IL-6, interleukin 6; BSA, bovine serum albumine; CSF, cerebro spinal fluid

■ REFERENCES

(1) Jacobs, P.; Bissonnette, R.; Guenther, L. C. Socioeconomic Burden of Immune-Mediated Inflammatory Diseases - Focusing on Work Productivity and Disability. *J. Rheumatol.* **2011**, *88*, 55−61.

(2) Carter, M. J.; Fish, M.; Jennings, A.; Doores, K. J.; Wellman, P.; Seow, J.; Acors, S.; Graham, C.; Timms, E.; Kenny, J.; Neil, S.; Malim, M. H.; Tibby, S. M.; Shankar-Hari, M. Peripheral Immunophenotypes in Children with Multisystem Inflammatory Syndrome Associated with SARS-CoV-2 Infection. *Nat. Med.* **2020**, *26*. DOI: 10.1038/s41591-020-1054-6.

(3) Slavich, G. M.; Irwin, M. R. From Stress to Inflammation and Major Depressive Disorder: A Social Signal Transduction Theory of Depression. *Psychol. Bull.* **2014**, *140*, 774−815.

(4) Miller, A. H.; Raison, C. L. The Role of Inflammation in Depression: From Evolutionary Imperative to Modern Treatment Target. *Nat. Rev. Immunol.* **2015**, *16*, 22.

(5) Baumeister, D.; Akhtar, R.; Ciufolini, S.; Pariante, C. M.; Mondelli, V. Childhood Trauma and Adulthood Inflammation: A Meta-Analysis of Peripheral C-Reactive Protein, Interleukin-6 and Tumour Necrosis Factor-α. *Mol. Psychiatry* **2016**, *21*, 642−649.

(6) Mehta, P.; McAuley, D. F.; Brown, M.; Sanchez, E.; Tattersall, R. S.; Manson, J. J. COVID-19: Consider Cytokine Storm Syndromes and Immunosuppression. *Lancet* **2020**, *395*, 1033−1034.

(7) Russell, B.; Moss, C.; George, G.; Santaolalla, A.; Cope, A.; Papa, S.; Van Hemelrijck, M. Associations between Immune-Suppressive and Stimulating Drugs and Novel COVID-19—a Systematic Review of Current Evidence. *Ecancermedicalscience* **2020**, *14*, 1022.

(8) Mukhopadhyay, S.; Hoidal, J. R.; Mukherjee, T. K. Role of TNFα in Pulmonary Pathophysiology. *Respir. Res.* **2006**, *7*, 125−134.

(9) Yndestad, A.; Kristian Damås, J.; Øie, E.; Ueland, T.; Gullestad, L.; Aukrust, P. Systemic Inflammation in Heart Failure - The Whys and Wherefores. *Heart Failure Rev.* **2006**, *11*, 83−92.

(10) Kumar, S.; Tripathy, S.; Jyoti, A.; Singh, S. G. Recent Advances in Biosensors for Diagnosis and Detection of Sepsis: A Comprehensive Review. *Biosens. Bioelectron.* **2019**, *124*−*125*, 205−215.
(11) Liu, G.; Qi, M.; Hutchinson, M. R.; Yang, G.; Goldys, E. M. Recent Advances in Cytokine Detection by Immunosensing. *Biosens. Bioelectron.* **2016**, *79*, 810−821.
(12) Bari, S. M. I.; Reis, L. G.; Nestorova, G. G. Calorimetric Sandwich-Type Immunosensor for Quantification of TNF-α. *Biosens. Bioelectron.* **2019**, *126*, 82−87.
(13) Huang, J.; Harvey, J.; Fam, W. H. D.; Nimmo, M. A.; Tok, I. Y. A. Novel Biosensor for Interleukin-6 Detection. *Procedia Eng.* **2013**, *60*, 195−200.
(14) Munje, R. D.; Muthukumar, S.; Jagannath, B.; Prasad, S. A New Paradigm in Sweat Based Wearable Diagnostics Biosensors Using Room Temperature Ionic Liquids (RTILs). *Sci. Rep.* **2017**, *7*, 1950.
(15) Filik, H.; Avan, A. A. Electrochemical Immunosensors for the Detection of Cytokine Tumor Necrosis Factor Alpha: A Review. *Talanta* **2020**, *211*, 120758.
(16) Hao, Z.; Wang, Z.; Li, Y.; Zhu, Y.; Wang, X.; De Moraes, C. G.; Pan, Y.; Zhao, X.; Lin, Q.; Lin, Q. Measurement of Cytokine Biomarkers Using an Aptamer-Based Affinity Graphene Nanosensor on a Flexible Substrate toward Wearable Applications. *Nanoscale* **2018**, *10*, 21681−21688.
(17) Pohanka, M. Piezoelectric Biosensor for the Determination of Tumor Necrosis Factor Alpha. *Talanta* **2018**, *178*, 970−973.
(18) Bellagambi, F. G.; Baraket, A.; Longo, A.; Vatteroni, M.; Zine, N.; Bausells, J.; Fuoco, R.; Di Francesco, F.; Salvo, P.; Karanasiou, G. S.; Fotiadis, D. I.; Menciassi, A.; Errachid, A. Electrochemical Biosensor Platform for TNF-α Cytokines Detection in Both Artificial and Human Saliva: Heart Failure. *Sens. Actuators, B* **2017**, *251*, 1026−1033.
(19) Chuang, H.-S.; Chen, Y.-J.; Cheng, H.-P. Enhanced Diffusometric Immunosensing with Grafted Gold Nanoparticles for Detection of Diabetic Retinopathy Biomarker Tumor Necrosis Factor-α. *Biosens. Bioelectron.* **2018**, *101*, 75−83.
(20) Sekine, Y.; Kim, S. B.; Zhang, Y.; Bandodkar, A. J.; Xu, S.; Choi, J.; Irie, M.; Ray, T. R.; Kohli, P.; Kozai, N.; Sugita, T.; Wu, Y.; Lee, K.; Lee, K.-T.; Ghaffari, R.; Rogers, J. A. A Fluorometric Skin-Interfaced Microfluidic Device and Smartphone Imaging Module for: In Situ Quantitative Analysis of Sweat Chemistry. *Lab Chip* **2018**, *18*, 2178−2186.
(21) Alizadeh, A.; Burns, A.; Lenigk, R.; Gettings, R.; Ashe, J.; Porter, A.; McCaul, M.; Barrett, R.; Diamond, D.; White, P.; Skeath, P.; Tomczak, M. A Wearable Patch for Continuous Monitoring of Sweat Electrolytes during Exertion. *Lab Chip* **2018**, *18*, 2632−2641.
(22) Lee, G.; Lee, J.; Kim, J.; Choi, H. S.; Kim, J.; Lee, S.; Lee, H. Single Microfluidic Electrochemical Sensor System for Simultaneous Multi-Pulmonary Hypertension Biomarker Analyses. *Sci. Rep.* **2017**, *7*, 7545.
(23) Mata, A.; Fleischman, A. J.; Roy, S. Characterization of Polydimethylsiloxane (PDMS) Properties for Biomedical Micro/Nanosystems. *Biomed. Microdevices* **2005**, *7*, 281−293.
(24) Goddard, J. M.; Hotchkiss, J. H. Polymer Surface Modification for the Attachment of Bioactive Compounds. *Prog. Polym. Sci.* **2007**, *32*, 698−725.
(25) Zhou, J. Surface Modification of Poly(dimethylsiloxane) (PDMS) for Microfluidic Devices. PhD Thesis, Flinders University, 2012.
(26) Orhan, J.-B.; Parashar, V. K.; Flueckiger, J.; Gijs, M. A. M. Internal Modification of Poly(Dimethylsiloxane) Microchannels with a Borosilicate Glass Coating. *Langmuir* **2008**, *24*, 9154−9161.
(27) Henares, T. G.; Mizutani, F.; Hisamoto, H. Current Development in Microfluidic Immunosensing Chip. *Anal. Chim. Acta* **2008**, *611*, 17−30.
(28) Zhang, F.-T.; Xu, L.; Chen, J.-H.; Zhao, B.; Fu, X.-Z.; Sun, R.; Chen, Q.; Wong, C.-P. Electroless Deposition Metals on Poly-(Dimethylsiloxane) with Strong Adhesion As Flexible and Stretchable Conductive Materials. *ACS Appl. Mater. Interfaces* **2018**, *10*, 2075−2082.
(29) Sunkara, V.; Cho, Y.-K. Investigation on the Mechanism of Aminosilane-Mediated Bonding of Thermoplastics and Poly-(Dimethylsiloxane). *ACS Appl. Mater. Interfaces* **2012**, *4*, 6537−6544.
(30) Ren, Y.; Huang, S.-H.; Mosser, S.; Heuschkel, M.; Bertsch, A.; Fraering, P.; Chen, J.-J.; Renaud, P. A Simple and Reliable PDMS and SU-8 Irreversible Bonding Method and Its Application on a Microfluidic-MEA Device for Neuroscience Research. *Micromachines* **2015**, *6*, 1923−1934.
(31) Yang, L.; Li, L.; Tu, Q.; Ren, L.; Zhang, Y.; Wang, X.; Zhang, Z.; Liu, W.; Xin, L.; Wang, J. Photocatalyzed Surface Modification of Poly(Dimethylsiloxane) with Polysaccharides and Assay of Their Protein Adsorption and Cytocompatibility. *Anal. Chem.* **2010**, *82*, 6430−6439.
(32) Khnouf, R.; Karasneh, D.; Albiss, B. A. Protein Immobilization on the Surface of Polydimethylsiloxane and Polymethyl Methacrylate Microfluidic Devices. *Electrophoresis* **2016**, *37*, 529−535.
(33) Chuah, Y. J.; Kuddannaya, S.; Lee, M. H. A.; Zhang, Y.; Kang, Y. The Effects of Poly(Dimethylsiloxane) Surface Silanization on the Mesenchymal Stem Cell Fate. *Biomater. Sci.* **2015**, *3*, 383−390.
(34) Gokaltun, A.; Yarmush, M. L.; Asatekin, A.; Usta, O. B. Recent Advances in Nonbiofouling PDMS Surface Modification Strategies Applicable to Microfluidic Technology. *Technol.* **2017**, *05*, 1−12.
(35) Vashist, S. K.; Lam, E.; Hrapovic, S.; Male, K. B.; Luong, J. H. T. Immobilization of Antibodies and Enzymes on 3-Aminopropyltriethoxysilane-Functionalized Bioanalytical Platforms for Biosensors and Diagnostics. *Chem. Rev.* **2014**, *114*, 11083−11130.
(36) Sui, G.; Wang, J.; Lee, C.-C.; Lu, W.; Lee, S. P.; Leyton, J. V.; Wu, A. M.; Tseng, H.-R. Solution-Phase Surface Modification in Intact Poly(Dimethylsiloxane) Microfluidic Channels. *Anal. Chem.* **2006**, *78*, 5543−5551.
(37) Khodakov, D. A.; Thredgold, L. D.; Lenehan, C. E.; Andersson, G. A.; Kobus, H.; Ellis, A. V. Surface Modification of Poly-(Dimethylsiloxane) (PDMS) Microchannels with DNA Capture-Probes for Potential Use in Microfluidic DNA Analysis Systems. In *Smart Nano−Micro Materials and Devices*; Society of Photo-Optical Instrumentation Engineers, 2011; Vol. *8204*, p 82040J.
(38) Ammar, M.; Smadja, C.; Giang Thi Phuong, L.; Azzouz, M.; Vigneron, J.; Etcheberry, A.; Taverna, M.; Dufour-Gergam, E. A New Controlled Concept of Immune-Sensing Platform for Specific Detection of Alzheimer's Biomarkers. *Biosens. Bioelectron.* **2013**, *40*, 329−335.
(39) Petreto, A.; Cardoso Dos Santos, M.; Lefebvre, O.; Ribeiro Dos Santos, G.; Ponzellini, P.; Garoli, D.; De Angelis, F.; Ammar, M.; Hildebrandt, N. Optimizing FRET on Aluminum Surfaces via Controlled Attachment of Fluorescent Dyes. *ACS Omega* **2018**, *3*, 18867−18876.
(40) Gunda, N. S. K.; Singh, M.; Norman, L.; Kaur, K.; Mitra, S. K. Optimization and Characterization of Biomolecule Immobilization on Silicon Substrates Using (3-Aminopropyl)Triethoxysilane (APTES) and Glutaraldehyde Linker. *Appl. Surf. Sci.* **2014**, *305*, 522−530.
(41) Séguin, C.; McLachlan, J. M.; Norton, P. R.; Lagugné-Labarthet, F. Surface Modification of Poly(Dimethylsiloxane) for Microfluidic Assay Applications. *Appl. Surf. Sci.* **2010**, *256*, 2524−2531.
(42) Fadeev, A. Y.; McCarthy, T. J. Self-Assembly Is Not the Only Reaction Possible between Alkyltrichlorosilanes and Surfaces: Monomolecular and Oligomeric Covalently Attached Layers of Dichloro- and Trichloroalkylsilanes on Silicon. *Langmuir* **2000**, *16*, 7268−7274.
(43) Baranowska, M.; Slota, A. J.; Eravuchira, P. J.; Alba, M.; Formentin, P.; Pallarès, J.; Ferré-Borrull, J.; Marsal, L. F. Protein Attachment to Silane-Functionalized Porous Silicon: A Comparison of Electrostatic and Covalent Attachment. *J. Colloid Interface Sci.* **2015**, *452*, 180−189.
(44) Beal, J. H. L.; Bubendorfer, A.; Kemmitt, T.; Hoek, I.; Mike Arnold, W. A Rapid, Inexpensive Surface Treatment for Enhanced Functionality of Polydimethylsiloxane Microfluidic Channels. *Biomicrofluidics* **2012**, *6*, 36503.

https://dx.doi.org/10.1021/acsabm.0c01188
ACS Appl. Bio Mater. 2021, 4, 1307−1318

(45) Wirth, M. J.; Fairbank, R. W. P.; Fatunmbi, H. O. Mixed Self-Assembled Monolayers-in Chemical Separations. *Science* **1997**, *275*, 44−47.
(46) Ulman, A. *An Introduction to Ultrathin Organic Films: From Langmuir-Blodgett to Self-Assembly*; Academic Press, 2013.
(47) Laborie, E.; Lefebvre, O.; Petreto, A.; Do Valé, M.; Smadja, C.; Dufour-Gergam, E.; Ammar, M. Highly Controlled Chemical Functionalization of PDMS Films. In *2019 Symposium on Design, Test, Integration & Packaging of MEMS and MOEMS*, 2019.
(48) End Note: Anti-porcin Antibodies Were Used Instead of Anti-human, Human and Pig Sharing 80% of Their Genome 10.1016/j.tim.2011.11.002.
(49) Séguin, C.; McLachlan, J. M.; Norton, P. R.; Lagugné-Labarthet, F. Surface Modification of Poly(Dimethylsiloxane) for Microfluidic Assay Applications. *Appl. Surf. Sci.* **2010**, *256*, 2524−2531.
(50) Rothka, J.; Studd, R.; Tate, K.; Timpe, D. *Outgassing of Silicone Elastomers*; ARLON—Silicone Technology Division, 2002.
(51) Villa, S.; Riani, P.; Locardi, F.; Canepa, F. Functionalization of Fe3O4 NPs by Silanization: Use of Amine (APTES) and Thiol (MPTMS) Silanes and Their Physical Characterization. *Materials* **2016**, *9*, 826.
(52) Regehr, K. J.; Domenech, M.; Koepsel, J. T.; Carver, K. C.; Ellison-Zelski, S. J.; Murphy, W. L.; Schuler, L. A.; Alarid, E. T.; Beebe, D. J. Biological Implications of Polydimethylsiloxane-Based Microfluidic Cell Culture. *Lab Chip* **2009**, *9*, 2132−2139.
(53) Hermanson, G. T. *Bioconjugate Techniques*, 3rd ed.; Elsevier, 2013.
(54) Morra, M.; Occhiello, E.; Marola, R.; Garbassi, F.; Humphrey, P.; Johnson, D. On the Aging of Oxygen Plasma-Treated Polydimethylsiloxane Surfaces. *J. Colloid Interface Sci.* **1990**, *137*, 11.
(55) Fritz, J. L.; Owen, M. J. Hydrophobic Recovery of Plasma-Treated Polydimethylsiloxane. *J. Adhes.* **1995**, *54*, 33−45.
(56) Hillborg, H.; Tomczak, N.; Olàh, A.; Schönherr, H.; Vancso, G. J. Nanoscale Hydrophobic Recovery: A Chemical Force Microscopy Study of UV/Ozone-Treated Cross-Linked Poly(Dimethylsiloxane). *Langmuir* **2004**, *20*, 785−794.
(57) Zargar, R.; Nourmohammadi, J.; Amoabediny, G. Preparation, Characterization, and Silanization of 3D Microporous PDMS Structure with Properly Sized Pores for Endothelial Cell Culture. *Biotechnol. Appl. Biochem.* **2016**, *63*, 190−199.
(58) Siddique, A.; Meckel, T.; Stark, R. W.; Narayan, S. Improved Cell Adhesion under Shear Stress in PDMS Microfluidic Devices. *Colloids Surf., B* **2017**, *150*, 456−464.
(59) Hillborg, H.; Ankner, J. F.; Gedde, U. W.; Smith, G. D.; Yasuda, H. K.; Wikström, K. Crosslinked Polydimethylsiloxane Exposed to Oxygen Plasma Studied by Neutron Reflectometry and Other Surface Specific Techniques. *Polymer* **2000**, *41*, 6851−6863.
(60) Goldstein, J.; Newbury, D. E.; Joy, D. C.; Lyman, C. E.; Echlin, P.; Lifshin, E.; Sawyer, L.; Michael, J. R. *Scanning Electron Microscopy and X-Ray Microanalysis*; Springer: US, 2003.
(61) Ishida, H. A Review of Recent Progress in the Studies of Molecular and Microstructure of Coupling Agents and Their Functions in Composites, Coatings and Adhesive Joints. *Polym. Compos.* **1984**, *5*, 101−123.
(62) Zhu, M.; Lerum, M. Z.; Chen, W. How to Prepare Reproducible, Homogeneous, and Hydrolytically Stable Aminosilane-Derived Layers on Silica. *Langmuir* **2012**, *28*, 416−423.
(63) Piruska, A.; Nikcevic, I.; Lee, S. H.; Ahn, C.; Heineman, W. R.; Limbach, P. A.; Seliskar, C. J. The Autofluorescence of Plastic Materials and Chips Measured under Laser Irradiation. *Lab Chip* **2005**, *5*, 1348−1354.
(64) Pasternack, R. M.; Rivillon Amy, S.; Chabal, Y. J. Attachment of 3-(Aminopropyl)Triethoxysilane on Silicon Oxide Surfaces: Dependence on Solution Temperature. *Langmuir* **2008**, *24*, 12963−12971.
(65) Long, D. A. *Infrared and Raman Characteristic Group Frequencies. Tables and Charts*, 3rd ed.; Socrates, G., Ed.; John Wiley and Sons, Ltd: Chichester, 2001; Vol. 35.
(66) Kim, J.; Seidler, P.; Wan, L. S.; Fill, C. Formation, Structure, and Reactivity of Amino-Terminated Organic Films on Silicon Substrates. *J. Colloid Interface Sci.* **2009**, *329*, 114−119.
(67) Deka, C.; Lehnert, B. E.; Lehnert, N. M.; Jones, G. M.; Sklar, L. A.; Steinkamp, J. A. Analysis of Fluorescence Lifetime and Quenching of FITC-Conjugated Antibodies on Cells by Phase-Sensitive Flow Cytometry. *Cytometry* **1996**, *25*, 271−279.
(68) End Note: LOD Calculated with Three Times the Standard Deviations from the Background Signal Obtained for the Blank in Absence of TNF-α Divided by the Slope of the Standard Curve https://www.ema.europa.eu/en/documents/scientific-guideline/ich-q-2-r1-validation-analytical-procedures-text-methodology-step-5_en.pdf.
(69) Cohen, N.; Sabhachandani, P.; Golberg, A.; Konry, T. Approaching near Real-Time Biosensing: Microfluidic Microsphere Based Biosensor for Real-Time Analyte Detection. *Biosens. Bioelectron.* **2015**, *66*, 454−460.
(70) Cizza, G.; Marques, A. H.; Eskandari, F.; Christie, I. C.; Torvik, S.; Silverman, M. N.; Phillips, T. M.; Sternberg, E. M. Elevated Neuroimmune Biomarkers in Sweat Patches and Plasma of Premenopausal Women with Major Depressive Disorder in Remission: The POWER Study. *Biol. Psychiatry* **2008**, *64*, 907−911.

https://dx.doi.org/10.1021/acsabm.0c01188
ACS Appl. Bio Mater. 2021, 4, 1307−1318